THE ROTATIONAL BEHAVIOR OF THE WHITE DWARF IN DQ HERCULIS: THE TURN-OVER SCENARIO

V. S. Geroyannis and P. J. Papasotiriou
Astronomy Laboratory, Department of Physics, University of Patras, GR-26500, Patras, Greece

Abstract

We compute axisymmetric models (i.e., their magnetic symmetry axis coincides with their rotation axis) simulating the DQ Her white dwarf. Our numerical results show that all the models computed are susceptible to "turn-over" (i.e., their magnetic symmetry axis gets inclining at a progressively increasing angle with respect to their invariant angular momentum axis up to the perpendicular position; this terminal configuration is known as "perpendicular rotator"). Consequently, DQ Her is either in its turn-over phase, or it is (an almost) perpendicular rotator. Assuming the first case (i.e., turn-over in progress), we compute the spin-down time rate of DQ Her due to turn-over (not to be confused with its spin-up time rate due to accretion) for several possible values of its magnetic field.

1 Introduction

The well-known nova DQ Herculis (N1934) is an eclipsing binary star, consisting of a white dwarf (the "primary star") and a late-type cool star (the "secondary star"), presumed to be in the main sequence (see, e.g., Patterson, 1994, hereafter P94). The mass of the white dwarf is about $0.60\,M_\odot$ (Horne, Welsh, & Wade, 1993) and its rotation period is about 142 s (see P94 and references therein; Zhang et al. 1995).

The white dwarf is spinning up with $\dot{P}_{\rm OBS} \simeq -8.1 \times 10^{-13}\,{\rm s\,s^{-1}}$ (Balachandran, Robinson, & Kepler 1983, § 3; Ritter 1985, hereafter R85, Table 1). This fast spin-up is caused by the combined action of accretion and magnetic field (see, e.g., R85; King & Lasota 1991; Warner & Wickramasinghe 1991).

In this paper we shall study the so-called "turn-over scenario" (Geroyannis, 2001, hereafter Paper I), according to which the DQ Her white dwarf is now undergoing a nonaxisymmetric transition from an initial axisymmetric differential rotation state to a terminal nonaxisymmetric rigid rotation state, due to turn-over of the magnetic symmetry axis with respect to the invariant angular momentum axis (coinciding, in turn, with the z axis). For clarity and convenience, we shall hereafter use the definitions and symbols of Paper I.

2 The turn-over scenario

According to the turn-over scenario, the DQ Her white dwarf undergoes three evolutionary phases. These phases can be easily understood in the plot of the central period, P, as a function of the angular momentum, L, for a constant-mass sequence of white dwarf models with mass, M, equal to the estimated mass of the DQ Her white dwarf.

In the "early evolutionary phase" the white dwarf can be described by an axisymmetric configuration, distorted by differential rotation and magnetic fields (both toroidal and poloidal). Due to the presence of the poloidal magnetic field, the white dwarf undergoes a secular angular momentum loss. In other words, we assume that the white dwarf was in the early past located at the point d of

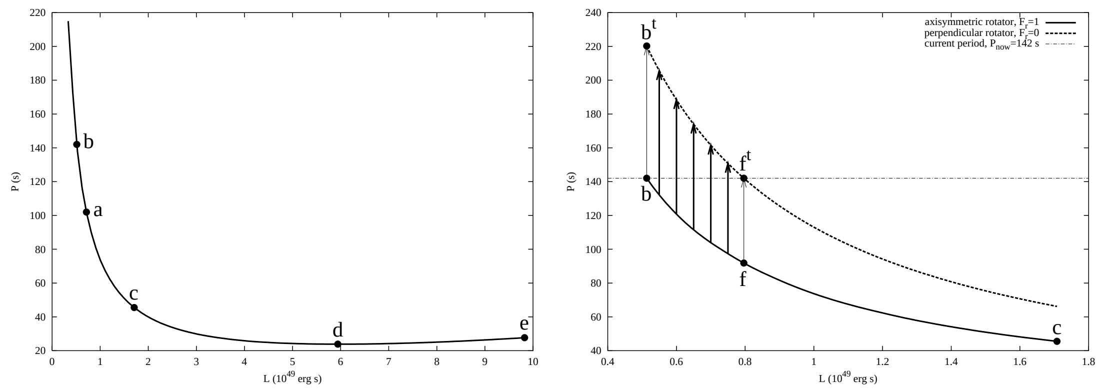

(a) Constant-mass sequence of white dwarf models with $M = 0.6 M_\odot$, $F_r = 1$, and $h = 0.08$. Point a: almost spherical model due to counterbalancing of the effects of rotation and poloidal field with the effects of toroidal field; point b: model with central period equal to the current period, $P_{\text{now}} = 142\,\text{s}$; point c: model for which $I_{33} = I_{11} = I_{22}$; point d: model with minimum central period ($dP/dL = 0$); point e: critically rotating model (the rightmost point of the curve).

(b) Magnification of Fig. 1(a) between points b and c (thick solid line), together with the $P(L)$ curve of the perpendicular rotator (thick dashed line). Thin horizontal dashed-dotted line: current period of DQ Her, $P = P_{\text{now}}$; point b^t: terminal model corresponding to the starting model b; point f^t: terminal model for which $P = P_{\text{now}}$; point f: starting model corresponding to the terminal model f^t. The thin arrow $b - b^t$ shows a turn-over just started; the thin arrow $f - f^t$ shows a turn-over just terminated. Thick arrows show possible turn-over scenarios currently in progress, which are studied numerically in this paper.

Figure 1: Plot of period at center, P, as a function of angular momentum, L, for (a) the axisymmetric rotator and (b) both the axisymmetric and the perpendicular rotator.

Fig. 1(a) (or near d, but to the left), where $dP/dL = 0$. Due to the secular angular momentum loss, the white dwarf is progressively moving to the left of the curve, leading to configurations with the same mass, but lower angular momentum and higher central period. The moment of inertia I_{33} along the rotation axis I_3 (which coincides with the magnetic symmetry axis and the z axis) is greater than the moments of inertia I_{11}, I_{22} ($I_{11} = I_{22}$) along the two other principal axes I_1 and I_2. However,the moment of inertia I_{33} is progressively decreased. At the point c of the curve, the moment of inertia I_{33} becomes equal to the moments of inertia I_{11} and I_{22}. After reaching that point, the white dwarf enters the “late evolutionary phase”, where continues loosing angular momentum and moving to the left of the curve, but now the configuration is in “dynamical asymmetry”, in the sense that the moment of inertia along the rotation axis is less than the moments of inertia along the two other principal axes, i.e., $I_{33} < I_{11} = I_{22}$. At some point s of the curve, the white dwarf enters the “turn-over phase”, where the dynamically asymmetric configuration turns over spontaneously, so that to subsequently rotate along axis with moment of inertia greater than I_{33}. The configuration becomes an “oblique rotator”, where the magnetic symmetry axis (coinciding with the I_3 principal axis) gets inclining at a progressively increasing “obliquity angle” or “turn-over angle”, χ, with respect to the invariant angular momentum axis. The oblique rotator generates a velocity field which carries mass elements across cylinders of different angular velocities and momenta via hydromagnetic Alfvén waves. The turn-over angle increases spontaneously up to $\chi \simeq 90°$, where the oblique rotator reaches its state of least energy, consistent with its prescribed angular momentum and magnetic field. In this terminal state, which is often called “perpendicular rotator”, differential rotation along the I_3 principal axis and all of its effects disappear. The excess energy, DE_{TOV}, due to the differential rotation field of motions is dissipated down to zero under the action of turbulent viscosity in the convective regions of the star. Thus, the perpendicular rotator is rotating rigidly along its I_1 principal axis, with rotational kinetic energy T_{RR} equal to $T_{\text{RR}} = T_{xx} - DE_{\text{TOV}}$, where T_{xx}

the rotational kinetic energy of the starting (differentially rotating) model. The final nonaxisymmetric state of the configuration is located at some point s^t in the $P\,(L)$ curve of the terminating, rigidly rotating, models (Fig 1(b)).

The reader can find a more detailed discussion about the turn-over scenario in Paper I; a detailed study of the internal dynamics of an oblique rotator can be found in Mestel & Takhar (1972).

3 The numerical method

The numerical method used to compute the constant-mass sequence of differentially rotating starting models is described in Geroyannis & Papasotiriou (2000). An almost complete set of quantities involved in the computations is given in Table 1 of Geroyannis & Papasotiriou (1999).

The average surface poloidal magnetic field, B_s, is somewhat prescribed to a value B_s^p by either the theory and the observations (see, e.g., King & Wynn 1999; Norton et al. 1999). We therefore examine seven "representative" values of B_s: $B_s = 5 \times 10^5, 2 \times 10^6, 3.5 \times 10^6, 5 \times 10^6, 6.5 \times 10^6, 8 \times 10^6, 9.5 \times 10^6$ G. These values are used to compute the corresponding poloidal magnetic parameter, β_*^p, using eq. [19] of Paper I.

An essential point concerning the turn-over scenario is that the toroidal magnetic field must be strong enough to induce dynamical asymmetry, while, on the other hand, it must be weak enough to permit angular momentum mixing via hydromagnetic Alfvén waves propagating across its field lines. An optimal value for the magnetic perturbation parameter, h, for which both conditions are satisfied, is found to be $h = 0.08$ (see Paper I, §§ 7-8 for details). We therefore take that value for the magnetic perturbation parameter of the starting model, h_{DR}, and, assuming that h remains constant during the turn-over phase, we also take the magnetic perturbation parameter of the terminal model, h_{RR}, equal to that value; i.e., $h_{\mathrm{DR}} = h_{\mathrm{RR}} = 0.08$.

Assuming that the turn-over phase of the DQ Her white dwarf is now in progress, the nonaxisymmetric transition should have started in the past, at some point between f and b in Fig. 1(b), since only in this region the present period $P_{\mathrm{now}} = 142\,\mathrm{s}$ can be achieved during the turn-over phase. Our numerical results concern five such points, with angular momenta L_{xx} of the starting axisymmetric models equal to $L_{xx} = 5.5 \times 10^{48}, 6 \times 10^{48}, 6.5 \times 10^{48}, 7 \times 10^{48}, 7.5 \times 10^{48}$ erg s. Thus, we examine five cases of L_{xx} for seven cases of B_s each, i.e., $5 \times 7 = 35$ possible turn-over phases currently in progress. In all cases, the differential rotation strength, F_r, is taken to be $F_r = 1$ (the maximum possible value).

Parameters concerning the turn-over phase are computed as in Paper I (see, especially, § 6 for the computation of the turn-over timescale, t_{TOV}).

4 Results and discussion

Our numerical results reveal that the turn-over timescale, t_{TOV}, varies from 4.3 million to 5.6 billion years, dependent on the angular momentum and the average surface poloidal magnetic field of the starting model. The corresponding turn-over angles vary from 30.5° to 80.9°.

A point of particular interest is the estimated values for the turn-over spin-down, $\dot{P}_{\mathrm{TOV}}$, which vary from $4.1 \times 10^{-16}\,\mathrm{s\,s^{-1}}$ to $3.9 \times 10^{-13}\,\mathrm{s\,s^{-1}}$. As already stated, the observed time rate of the central period is $\dot{P}_{\mathrm{OBS}} \simeq -8.1 \times 10^{-13}\,\mathrm{s\,s^{-1}}$, i.e., the white dwarf is now spinning up. Our numerical results reveal that, for "low" values of the surface poloidal magnetic field, the turn-over spin-down is totally screened by the accretional spin-up, since $\dot{P}_{\mathrm{TOV}} \ll |\dot{P}_{\mathrm{OBS}}|$. However, higher values of the

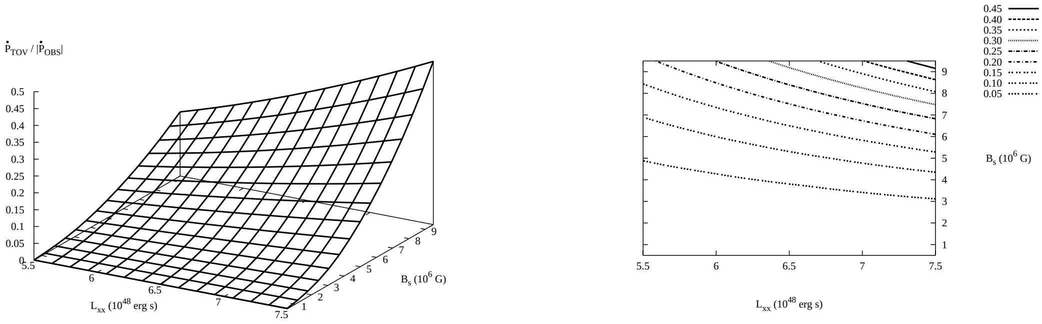

(a) 3D plot.

(b) Contour plot.

Figure 2: The ratio $\dot{P}_{\mathrm{TOV}}/|\dot{P}_{\mathrm{OBS}}|$ as a function of L_{xx} and B_s.

surface poloidal magnetic field lead to values of $\dot{P}_{\mathrm{TOV}}$ which are comparable to $|\dot{P}_{\mathrm{OBS}}|$ (Fig. 2). This holds true for turn-over processes near their end (high values of L_{xx}), as well as turn-over processes started "recently" (low values of L_{xx}). In other words, if the surface poloidal magnetic field is weak, the observed time rate of the central period is caused mainly by the accretional activities of the binary system, and the turn-over effects are negligible, as far as $\dot{P}$ is concerned; on the other hand, if the surface poloidal magnetic field is strong or even moderate, the turn-over effects to the time rate of the central period cannot be neglected.

Acknowledgments

The research reported here was supported by the Research Committee of the University of Patras (C. Carathéodory's Research Project 1998/1932).

References

Balachandran, S., Robinson, E. L., & Kepler, S. O. 1983, *PASP*, 95, 653
Geroyannis, V. S. 2001, *astro-ph/0103080* (Paper I)
Geroyannis, V. S., & Papasotiriou, P. J. 1999, *ApJS*, 121, 219
Geroyannis, V. S., & Papasotiriou, P. J. 2000, *ApJ*, 534, 359
Horne, K., Welsh, W. F., & Wade, R. A. 1993, *ApJ*, 410, 357
King, A. R., & Lasota, J-P. 1991, *ApJ*, 378, 674
King, A. R., & Wynn, G. A. 1999, *MNRAS*, 310, 203
Mestel, L., & Takhar, H. S. 1972, *MNRAS*, 156, 419
Norton, A. J., Beardmore, A. P., Allan, A., & Hellier, C. 1999, *A&A*, 347, 203
Patterson, J. 1994, *PASP*, 106, 209 (P94)
Ritter, H. 1985, *A&A*, 148, 207 (R85)
Warner, B., & Wickramasinghe, D. T. 1991, *MNRAS*, 248, 370
Zhang, E., Robinson, E. L., Stiening, R. F., & Horne, K. 1995, *ApJ*, 454, 447